This article has been accepted for publication in a future issue of this journal, but has not been fully edited. Content may change prior to final publication. Citation information: DOI 10.1109/LAWP.2018.2870098, IEEE Antennas and Wireless Propagation Letters

3D printed Horn Antennas and Components Performance for Space and Telecommunications

Jorge Teniente, Juan Carlos Iriarte, Rubén Caballero, Daniel Valcázar, Mikel Goñi and Aitor Martínez

***Abstract*—In this work, a study of the performance of several antennas and components, manufactured using an accurate stereolithography 3D printer and resin for maximum accuracy and detail, is carried out. Electroless plating of the components to cover the pieces with a thick copper layer to improve their mechanical resistance is undertaken. Several SatCom horn antennas and components are designed, manufactured, and tested. A detailed study of a spline horn antenna and a filter is covered. These results are compared to the metallic lathe manufactured versions. Conclusions are derived from these tests, which are useful to improve additive manufactured components in future versions.**

***Index Terms*—Additive manufacturing, electroless plating, horn antenna, surface roughness.**

I. Introduction

Additive manufacturing technologies, often known as 3D printing, are being used nowadays in an increasing number of applications. However, the technology needs further research and development to find better solutions that fit our needs.

Additive manufacturing is not a new technology, but it has become popular in recent years since 3D printers are now more affordable, accurate and reliable. In fact, 3D printing for high frequency antennas and components, as scientific literature exhibits [1-3], is becoming an interesting tool for antennas and RF/Microwave waveguide hardware. In this specific sector, additive manufacturing is making it possible to produce complex, single-piece, lightweight parts that would be challenging or even impossible to achieve using the classical milling process, but the metallization of such complex structures is still difficult.

It would be interesting to 3D print the needed pieces in metal as is described in [4-6]. The main benefit of this technique is that it produces robust parts; however, the accuracy, surface roughness and conductivity of metallic additive manufacturing needs to be further developed, and could possibly demand post-processing steps such as polishing or milling.

Usually the best results come from the 3D printing of precise plastic parts by means of stereolithography [7], thus needing an additional metallization step. The simplest way to achieve this is to manufacture the device in a split-block configuration and apply a metal layer afterwards by physical vapor deposition (PVD) or electroplating [8-11]. Nevertheless, both blocks need to be attached, screwed together, and properly aligned; this technique sacrifices the flexibility of monolithic devices.

Nevertheless, some authors have found ways to metallize intricate inner parts [1-3], [12, 13] and have developed a metallization technique (based on electroless plating) that can produce a uniform layer of metal on top of the inner surfaces of a monolithically printed plastic part, thus obtaining highly accurate, lightweight, and low insertion loss devices. In this paper, we are trying to replicate such performances with a different approach, based on high performance stereolithography 3D printed antennas and components for SatCom, and applying a thick electroless plating copper metallization to reduce roughness and increase mechanical robustness.

II. Selection of Space and Telecommunications components

A wide variety of components were designed, manufactured, and tested to have a comprehensive knowledge of the technology. These components include waveguides, filters, diplexers, orthomode transducers and horn antennas. Some horn antennas that operate at higher frequencies, far from SatCom frequencies, were tested to evaluate their performance. Most of the components were manufactured in one piece since splitting is to be avoided. This means that the metallization of the inner parts must be good enough to not affect the electric performance of the components.

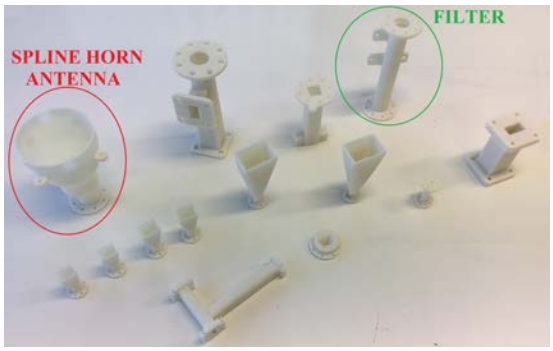

Fig. 1. Manufactured components after being 3D printed and processed. Spline horn antenna and filter are indicated in the picture.

In Figs.1 and 2 some of these manufactured components can be seen before and after copper metallization.

A local company, Wehl & Partner Iberica Rapid Prototyping S.L., manufactured these components with an accurate stereolithography 3D printer using Somos® PerFORM resin for maximum accuracy and details. Somos® PerFORM produces strong, stiff, high temperature

Manuscript received March 31, 2018.

This work was supported by the Spanish Ministry of Economy and Competitiveness, under Project TEC2016-76997-C3-1-R-DIDACTIC and the Navarra Government under European Union's Horizon 2020 research and innovation programme MANUNET under Project "New Manufacturing Techniques for Space and Telecommunications" (NEMACTEC-ST).

(Corresponding author: Jorge Teniente)

J. Teniente and J. C. Iriarte are with the Institute of Smart Cities and the Electrical, Electronic and Communication Engineering Department, Public University of Navarra, Campus de Arrosadía, E-31006 Pamplona, Spain (e-mail: jorge.teniente@unavarra.es, jcarlos.iriarte@unavarra.es).

R. Caballero, D. Valcázar, M. Goñi and A. Martínez are with ANTERAL S.L, Edificio I+D "Jerónimo de Ayanz", Campus de Arrosadía, E-31006 Pamplona, Spain (e-mail: rcaballero@anteral.com, valcazar@anteral.com, mgoni@anteral.com, aitor@anteral.com).

This article has been accepted for publication in a future issue of this journal, but has not been fully edited. Content may change prior to final publication. Citation information: DOI 10.1109/LAWP.2018.2870098, IEEE Antennas and Wireless Propagation Letters

resistant composite parts. The company does not disclose details about the 3D printer used and the process followed; according to them, the accuracy of the results depends more on the quality of the resin and the recipe used for manufacture than on the SLA 3D printer's resolution.

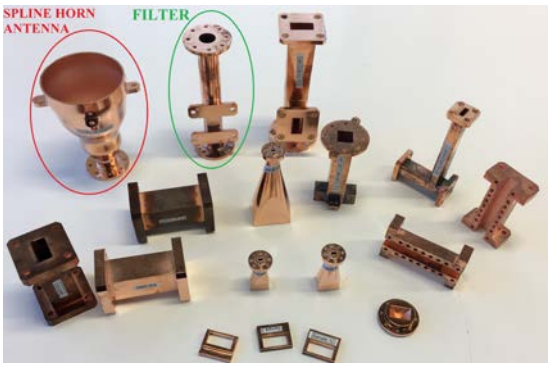

Fig. 2. Manufactured components after copper metallization. Spline horn antenna and filter are indicated in the picture.

The 3D printed components (see Fig. 1) are metallized by the same company employing an electroless plating procedure, achieving high quality copper plating with a final thickness between 100 and 150 μm, (see Fig. 2). The metallized components see their weight and mechanical resistance increase significantly because of the copper layer, making their behavior comparable to that of classically milled components.

In this research paper, two such manufactured components (a spline horn antenna and a circular waveguide iris coupled filter) are evaluated, since they are the ones which have presented better results. These results, although not perfect, have answered some of the questions regarding 3D printing issues for antennas and related components, and will serve to improve future designs.

III. 3D Printed SatCom Spline Horn Antenna performance

A compact spline horn antenna that is part of a Direct Radiating Array for SatCom was 3D printed, metallized with a thick copper layer and tested. Its profile, composed of 15 splines, can be seen in Fig. 3. The same horn antenna manufactured in aluminium with a lathe has also been tested to serve as a reference.

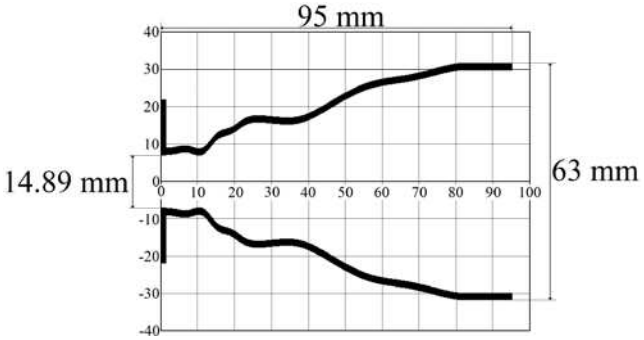

Fig. 3. Spline horn antenna profile.

This horn antenna presents a gain above 17 dB and a crosspolar level from -9 to 9 degrees below -30 dB maintaining a return loss above 25 dB between 12.95 and 14.85 GHz.

In Figs. 4, 5 and 6 the simulated and measured results of both versions of the spline horn antenna are shown. Measurements were done at UPNA anechoic chamber in a far field configuration with exactly the same set-up for both versions of the antenna, to allow for a perfect comparison.

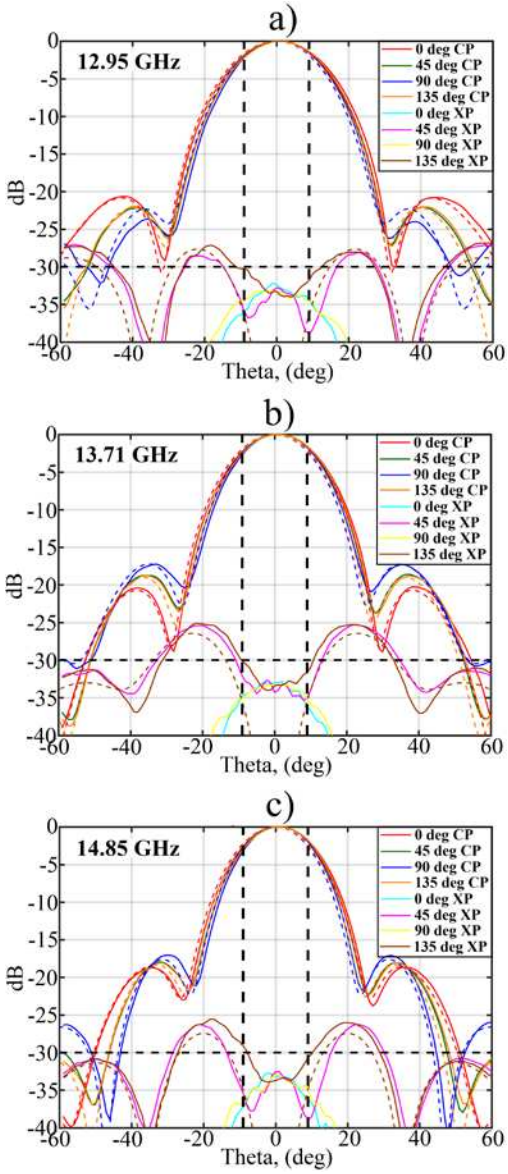

Fig. 4. Measured (solid lines) and simulated (dashed lines) far field radiation patterns for the main planes of the 3D printed spline horn antenna.
a) 12.95 GHz b) 13.71 GHz c) 14.85 GHz

From the measured results (see Figs. 4 and 5) it is remarkable that in both the 3D printed version and the metallic version there is a close agreement between the copolar patterns; it is difficult to find any differences between the 3D printed and metallic versions regarding this parameter.

With respect to the crosspolar radiation patterns, both horn antennas accomplish the crosspolar requirement from -9 to 9 degrees, but the metallic horn antenna exhibits better crosspolar level results. In any case, the main difference comes from the crosspolar level at boresight in the 0 and 90 degrees plane cuts.

In Fig. 4, it can be seen that the crosspolar level in the 0 and 90 degrees plane cuts reaches around -35 dB, whereas in Fig. 5, the crosspolar radiation in both planes is well below -40 dB. The crosspolar level of a symmetrical spline horn should be null at boresight, so this aspect means that the 3D printed horn antenna is not as symmetrical as the lathe manufactured one. In this case, it does not affect the required performance since this horn antenna is for a linear polarization application, but it should be considered for future improvements in 3D printed horn antennas.

This article has been accepted for publication in a future issue of this journal, but has not been fully edited. Content may change prior to final publication. Citation information: DOI 10.1109/LAWP.2018.2870098, IEEE Antennas and Wireless Propagation Letters

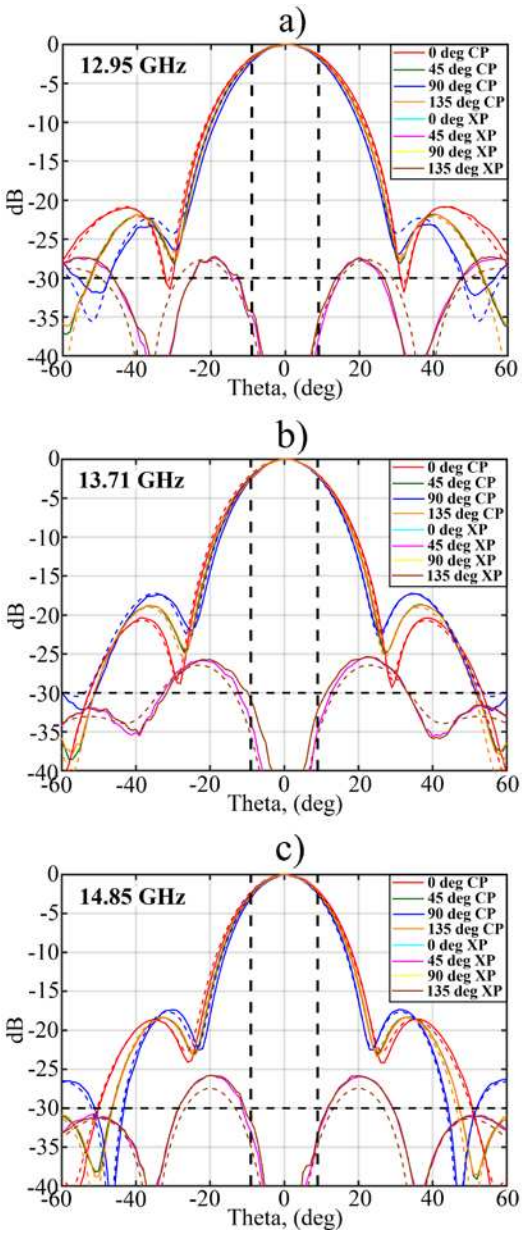

Fig. 5. Measured (solid lines) and simulated (dashed lines) far field radiation patterns for the main planes of the metallic spline horn antenna.
a) 12.95 GHz b) 13.71 GHz c) 14.85 GHz

The authors consider that this discrepancy in the crosspolar level in the 0 and 90 degrees planes for the 3D printed version of the spline horn antenna is due to slight differences in the layer-to-layer centre of manufacturing. The 3D printed spline horn antenna printing has been done following the propagation direction to take advantage of the structure's symmetry. This precision error is much lower in the lathe manufactured version, since in a lathe, the rotation of the metallic piece to be milled reduces this kind of asymmetry considerably.

In Fig. 6, simulated and measured directivity and gain for the spline horn antenna are plotted. Directivity has been calculated by means of integration of the radiation patterns given in Figs. 4 and 5. Only a slight difference (below 0.2 dB) can be seen between simulated and measured directivity results. The measured directivity is in fact slightly higher than simulated one since measured radiation pattern employed for this calculation ranged from -60 to 60 degrees assuming no radiation apart from that radiation cone.

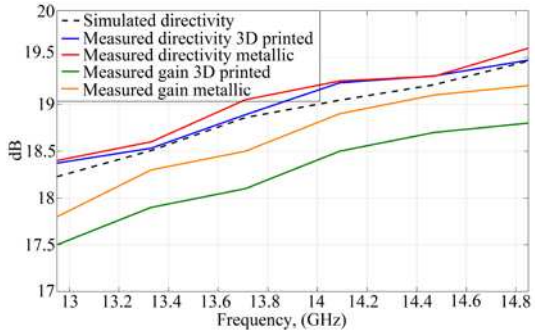

Fig. 6. Measured (solid lines) and simulated (dashed lines) directivity and measured gain of the 3D printed and metallic versions of the spline horn antenna.

Regarding gain, this parameter has been measured by the three-horn antenna substitution method employing a calibrated Flann Microwave standard gain horn. From Fig. 6 it can be concluded that both measured gain curves are below the directivity, indicating some losses, but the 3D printed spline horn has clearly lower gain results than those of the metallic spline horn.

After several years of calibration procedures at UPNA anechoic chamber, we can assume around ± 0.4 dB of uncertainty (95% confidence) in the three-horn antenna substitution method for gain measurement (including boresight maximum positioning inaccuracies, proximity effects, multipath interference, size differences between horn apertures and the calibration inaccuracy of the Flann Microwave standard gain horn employed) [12]. However, even assuming such gain measurement error, it is clear that the 3D printed spline horn exhibits higher losses than the lathe manufactured metallic spline horn.

These losses found in the measured gain can arise from conductivity of the metallic surface for both horns or from the surface roughness. Since the lathe manufactured horn is made in aluminium and the 3D printed horn is plated with a thick pure copper layer we can conclude that the losses come from surface roughness since the roughness of the 3D printed horn inside surface is clearly higher than the smooth surface of the lathe manufactured metallic horn. In section V, the measured roughness of the manufactured components are evaluated to try to answer to these evaluated losses.

IV. 3D Printed SatCom Circular Waveguide Iris-Coupled Filter performance

A circular waveguide high pass filter composed of 9 circular waveguide irises designed for SatCom has been designed and 3D printed. A lathe manufactured metallic version has also been manufactured to serve as reference. The 3D printed version has been plated with a thick copper plating, see Fig. 7.

Fig. 7. 3D printed SatCom circular waveguide filter measurement.

This article has been accepted for publication in a future issue of this journal, but has not been fully edited. Content may change prior to final publication. Citation information: DOI 10.1109/LAWP.2018.2870098, IEEE Antennas and Wireless Propagation Letters

This filter design presents a passband from 12.95 to 14.85 GHz coincident with the previously covered spline horn antenna bandwidth, and a stopband from 10 to 12.5 GHz with a rejection above 50 dB. Its measured results as well as its profile are depicted in Fig. 8. The resultant insertion loss in the passband is 0.4 dB for the 3D printed version compared to 0.05 dB for the metallic version. It is assumed that this high insertion loss is because of the surface roughness, this aspect will be further evaluated in section V.

In Fig. 8 a 250 MHz frequency displacement in the passband for the 3D printed version can be seen, but otherwise the metallic version presents an S parameter result very similar to the simulated one. This displacement is a consequence of the final 3D printed dimensions, which were modified by 125 μm to take the metallization thickness into account; but the result is that, because during the electroless plating method the fluids travelling inside its intricate parts were deposited forming a much thinner layer, the overall dimensions of the filter are smaller than expected.

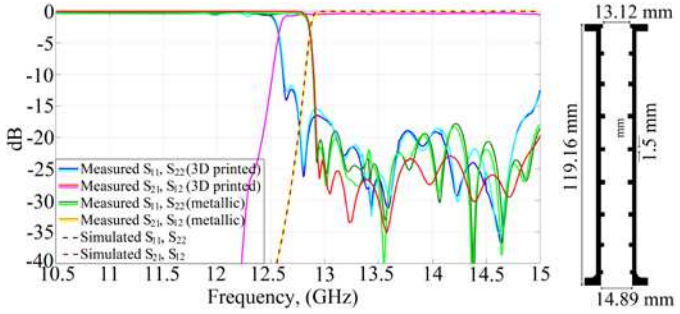

Fig. 8. Measured (solid lines) and simulated (dashed lines) results of the 3D printed and metallic SatCom circular waveguide iris-coupled filter versions. A caption includes the filter profile.

In Fig. 9, simulated results for nominal and 125 μm subtraction in inner dimensions are included to clarify this measured displacement that is clearly coincident with that of Fig. 8.

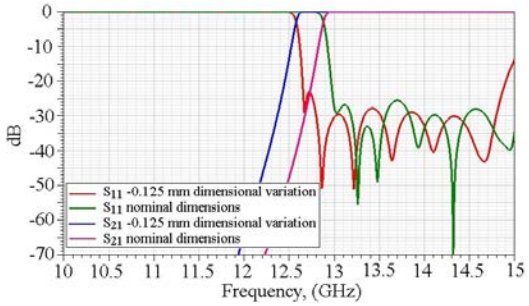

Fig. 9. Simulated results for the filter with nominal dimensions and with -125 μm inner dimensions modification.

V. Roughness Measurement of Manufactured Components

Surface roughness loss has a big effect when said roughness is comparable to skin depth. In any case, this loss is difficult to quantify, and there is not an exact calculation of its effect [13, 14]. The reason is that the geometry of the roughness is usually irregular and therefore hard to predict. It was deemed interesting to quantify the roughness of the 3D printed pieces before and after metallization, since it is likely the main reason for the losses in the studied components.

To measure the roughness, we have used a Mitutoyo SJ-410 roughness tester and to provide as accurate as possible value of the measured results, 10 different points have been evaluated for each of the pieces considered in this paper. Roughness has been measured for R_a and R_z parameters along 4 mm sampling lengths in the inner part of the components along the growth direction of the 3D printer. R_a is the arithmetical average value of all absolute distances of the roughness profile. R_z is the average maximum peak to valley of five consecutive sampling lengths within the measuring length. This means that the extreme values have a much greater influence on the final value of R_z than on R_a.

According to the scientific literature, surface roughness loss has a big effect when roughness is of the order of skin depth [13, 14]. If we calculate skin depth at 14 GHz, it is around 0.55 μm for pure copper (1.673 μΩ·cm bulk resistivity) and 0.7 μm for aluminium (2.65 μΩ·cm bulk resistivity). According to table I, surface roughness for the 3D printed components is at least 3 times than that of skin depth if we take R_a into account, and much worse if we take R_z into account. However, the surface roughness for the lathe manufactured versions is much lower. This result clearly shows that the surface roughness of the manufactured components is affecting the losses and should be taken into account in the manufacturing of 3D printed components.

TABLE I
Roughness of Manufactured Components

SatCom component	R_a (μm)	R_z (μm)
3D printed spline horn antenna before plating	1.80 μm	12.1 μm
3D printed spline horn antenna after plating	1.79 μm	10.7 μm
Lathe manufactured spline horn antenna	0.082 μm	0.5 μm
3D printed circular waveguide filter before plating	1.32 μm	8.6 μm
3D printed circular waveguide filter after plating	1.24 μm	7.9 μm
Lathe manufactured circular waveguide filter	0.096 μm	0.5 μm

From table I results, it can be appreciated that metallization reduces the surface roughness slightly and that such a reduction is more accentuated in R_z than in R_a. In any case, as the surface roughness of the stereolithography 3D printed components in the growing direction is above 1 μm, this value translates to the metallized versions, and although a thick metal layer is applied, such a thick layer doesn't improve the result. Several techniques are being investigated to improve surface roughness in 3D printed components. These investigations are based on a physical treatment (polishing of the inner 3D printed parts by means of a liquid flow containing tiny abrasive particles) and even chemical treatment using abrasive chemicals.

VI. Conclusion

3D printed horn antennas and components for SatCom have been evaluated in this paper. These components have been manufactured with a high precision stereolithography 3D printer in Somos® PerFORM resin for maximum accuracy and detail. The printed components have been metallized afterwards with a 100-150 μm thick copper layer.

A 3D printed spline horn antenna and a circular waveguide filter have been studied. The losses of both components are high compared to their equivalent lathe manufactured metallic versions. A study of the roughness of the 3D printed manufactured components answers such high loss result.

The 3D printed filter also presents a 250 MHz frequency displacement in its S parameter measured results. This frequency displacement is due to the manufacturing dimension change prior to 3D printing to take the thickness of the metallization layer into account, but the result is that the inner metallization layer is much thinner than anticipated.

This article has been accepted for publication in a future issue of this journal, but has not been fully edited. Content may change prior to final publication. Citation information: DOI 10.1109/LAWP.2018.2870098, IEEE Antennas and Wireless Propagation Letters

REFERENCES

[1] A. Macor, E. de Rijk, S. Alberti, T. Goodman, and J-Ph. Ansermet, "Three-dimensional stereolithography for millimeter wave and terahertz applications," Review of Scientific Instruments 83, 046103 (2012); DOI: 10.1063/1.3701738.

[2] A. von Bieren, E. de Rijk, J.-Ph. Ansermet, and A. Macor, " Monolithic metal-coated plastic components for mm-wave applications," 39th International Conference on Infrared, Millimeter, and Terahertz waves (IRMMW-THz), September 2014, DOI: 10.1109/IRMMW-THz.2014.6956222.

[3] A. I. Dimitriadis, T. Debogovic, M. Favre, M. Billod, L. Barloggio, J.-Ph. Ansermet, and E. de Rijk, "Polymer-Based Additive Manufacturing of High Performance Waveguide and Antenna Components," Proceedings of the IEEE, Vol.: 105, Issue: 4, April 2017, DOI: 10.1109/JPROC. 2016.2629511.

[4] B. Zhang and H. Zirath, "Metallic 3-d printed rectangular waveguides for millimeter-wave applications," IEEE Transactions on Components, Packaging and Manufacturing Technology, vol. 6, pp. 796–804, May 2016.

[5] M. Szymkiewicz, Y. Konkel, C. Hartwanger, and M. Schneider, "Kuband sidearm orthomode transducer manufactured by additive layer manufacturing," in 2016 10th European Conference on Antennas and Propagation (EuCAP), pp. 1–4, April 2016.

[6] M. D. Benge, R. C. Huck, and H. H. Sigmarsson, "X-band performance of three-dimensional, selectively laser sintered waveguides," in 2014 IEEE Antennas and Propagation Society International Symposium (APSURSI), pp. 13–14, July 2014.

[7] A. Gomez-Torrent, F. Teberio, I. Gómez López, J.M. Percaz, R. Caballero-Nagore, U. Beaskoetxea, A. Martinez, I. Arnedo, I. Maestrojuan, I. Arregui, G. Crespo, M. Beruete, T. Lopetegui1, M.A.G. Laso, J. Teniente, "A study of the additive manufacturing technology for RF/Microwave components," 11th European Conference on Antennas and Propagation, march 2017, DOI: 10.23919/EuCAP.2017.7928732

[8] M. D'Auria, W. J. Otter, J. Hazell, B. T. W. Gillatt, C. Long-Collins, N. M. Ridler, and S. Lucyszyn, "3-d printed metal-pipe rectangular waveguides," IEEE Transactions on Components, Packaging and Manufacturing Technology, vol. 5, pp. 1339–1349, Sept 2015.

[9] F. Cai, W. T. Khan, and J. Papapolymerou, "A low loss x-band filter using 3-d polyjet technology," in 2015 IEEE MTT-S International Microwave Symposium, pp. 1–4, May 2015.

[10] K. V. Hoel, S. Kristoffersen, J. Moen, K. G. Kjelg°ard, and T. S. Lande, "Broadband antenna design using different 3d printing technologies and metallization processes," in 2016 10th European Conference on Antennas and Propagation (EuCAP), pp. 1–5, April 2016.

[11] J. R. Montejo-Garai, I. O. Saracho-Pantoja, C. A. Leal-Sevillano, J. A. Ruiz-Cruz, and J. M. Rebollar, "Design of microwave waveguide devices for space and ground application implemented by additive manufacturing," in Electromagnetics in Advanced Applications (ICEAA), 2015 International Conference on, pp. 325–328, Sept 2015.

[12] A. I. Dimitriadis, M. Favre, M. Billod, J. P. Ansermet, and E. de Rijk, "Design and fabrication of a lightweight additive-manufactured ka-band horn antenna array," in 2016 10th European Conference on Antennas and Propagation (EuCAP), pp. 1–4, April 2016.

[13] X. Shang, P. Penchev, C. Guo, M. J. Lancaster, S. Dimov, Y. Dong, M. Favre, M. Billod, and E. de Rijk, "W -band waveguide filters fabricated by laser micromachining and 3-d printing," IEEE Transactions on Microwave Theory and Techniques, vol. 64, pp. 2572–2580, Aug 2016.

[12] G.T. Park, D. Bodner, D. Kremer, D. Musser, J. Snyder, D. B. Payne, and J. R. Stern, "Measured Error Terms for the Three-Antenna Gain-Measurement Technique," in Proc. AMTA 2000 22nd Annual Meeting and Symposium on Antenna Measurement Techniques Association, November 2000.

[13] G. Gold, and K. Helmreich, "A Physical Surface Roughness Model and Its Applications," in IEEE Transactions on Microwave Theory and Techniques, Vol. 65, No. 10, October 2017.

[14] M. Holmberg, D. Dancila, A. Rydberg, B. Hjörvarsson, U. Jansson, J. J. Marattukalam, N. Johansson and J Andersson, "On Surface Losses in Direct Metal Laser Sintering Printed Millimeter and Submillimeter Waveguides," in Journal of Infrared, Millimeter and Terahertz Waves, Vol. 39, Issue 6, pp. 535-545, June 2018; DOI: 10.1007/s10762-018-0470-x.